

Self-compression of spatially limited laser pulses in a system of coupled light-guides

A. A. Balakin,^{*} A. G. Litvak, V. A. Mironov, and S. A. Skobelev[†]
Institute of applied physics RAS, 603950 Nizhniy Novgorod, Russia
 (Dated: December 14, 2024)

The self-action features of wave packets propagating in a two-dimensional system of equidistantly arranged fibers are analytically and numerically studied on the basis of the discrete nonlinear Schrödinger equation. Self-consistent equations for the characteristic scales of a Gaussian wave packet are derived on the basis of the variational approach. A qualitative analysis of the self-action regimes has been carried out. The self-focusing of the wave beam and subsequent self-channeling of the radiation in the central light guide have been considered. The possibility of self-compression of soliton-like laser pulses in the process of three-dimensional wave packets self-focusing in a discrete optical fiber system with an anomalous dispersion of group velocity has been studied. Structural changes in the wave packet associated with the development of instabilities are considered numerically. In the case of wave packets with initial Gaussian shape, self-focusing and subsequent self-channeling of radiation is accompanied by the development of a modulation instability and the formation of a set of light bullets in the central fiber. In the regime of hollow wave beams, the filamentation instability becomes predominant. As a result, it becomes possible to form a set of light bullets in optical fibers located on the ring.

PACS numbers: 42.65.-k, 42.50.-p, 42.65.Jx

I. INTRODUCTION

One of the modern trends in fiber optics is associated with the possibility of using specially structured waveguide systems to control light fluxes [1, 2]. It is actively supported by technological progress in creating micro- and nano-heterogeneous structures. Photonic crystals and metamaterials, in which the optical refractive index is periodically modulated, are widely used [1–3]. At the same time, the nonlinear wave science in spatially periodic media active development. Due to the nonlinear nature of the interaction of optical radiation with the medium, the situation here turned out to be richer than in solid-state physics. In addition to the purely fundamental interest in the research, there is practical aspect: the possibilities of generating a supercontinuum [4] and shortening the durations of laser pulses [5, 6], controlling the structure of the wave field [7] and the formation of light bullets [8, 9], use active fiber systems for generation of intense laser pulses [10].

In a continuous medium, the basic model for study the wave field self-action is the nonlinear Schrödinger equation (NSE). The generalization of this model for describing the features of nonlinear processes in a system of weakly coupled fibers was successful [1–3, 11]. The discrete nonlinear Schrödinger equation (DNSE) is also widely used to study the dynamics of nonlinear excitations in solid state physics [12], in molecular systems [13] including those on the quantum level of the description of the medium. Due to the complexity of the processes accompanying the propagation of intense laser radiation in a spatially stratified medium, theoretical research relies

mainly on numerical simulation of the problem. It shows that even in the one-dimensional case discrete models demonstrate more complex behavior [1–3, 11–13] than in the continuous case. The use of approximate methods of studying the system dynamics makes it possible to classify characteristic regimes of self-action and to determine critical parameters. The most promising for this is the variational approach [14–16]. As in the case of NSE, one can obtain equations for changing the width of the wave field and the curvature of the phase front of Gaussian wave beams in a discrete problem along the propagation path. In this generalized aberration-free approximation, it is possible to describe not only the self-focusing of initially smooth field distributions up to the lattice size, but also the effects of the transition to the self-channeling mode of radiation in the central fiber [16], determined by the discrete nature of the medium.

The purpose of this paper is to study analytically and numerically the evolution of intense wave fields propagating along a two-dimensional system of light-guides. The structure of the paper is as follows. In the section II, equations of the aberration-free approximation are derived, using the variational approach. On the basis of these equations, a qualitative analysis of the modes of self-action of wave beams in a two-dimensional lattice is carried out, and features of self-compression of femtosecond soliton-like laser pulses in a discrete system are investigated. The section III presents results of numerical simulation of two-dimensional DNSE and shows good agreement with analytical analysis of the system dynamics at powers not much exceeding the critical power of self-focusing. Using the numerical simulation (section IV), a detailed picture of the self-focusing of the radiation in the central fiber, shortening and subsequent splitting of the laser pulse with further propagation of the wave field along the axis of the system is investigated. The

^{*} balakin.alexey@yandex.ru

[†] sksa@ufp.appl.sci-nnov.ru

possibility of forming a set of light bullets in the process of development of filamentation instability in the field of hollow wave beams is considered. In conclusion, the results of the work are summarized.

II. VARIATIONAL APPROACH

Let us consider a model in which the light-guides are located at the nodes (n, m) of a rectangular lattice. The envelope amplitude u_{nm} of the wave packet in the (n, m) waveguide changes during the propagation along the z axis under the action of the following factors: dispersion of the waveguide system, cubic nonlinearity of the medium, interaction with neighboring light-guides. This yields the discrete NSE of the following form [5, 6, 16]:

$$i\frac{\partial u_{n,m}}{\partial z} + \gamma\frac{\partial^2 u_{n,m}}{\partial \tau^2} + u_{n+1,m} + u_{n-1,m} + u_{n,m+1} + u_{n,m-1} + |u_{n,m}|^2 u_{n,m} = 0. \quad (1)$$

Here τ is the longitudinal coordinate of the wave packet, γ is the coefficient characterizing the quadratic dispersion of the group velocity of the light-guide. Further, we consider only the case of an anomalous dispersion of the group velocity ($\gamma = 1$). This equation has a Hamiltonian structure, like the continuous NSE. In addition, the system of equations (1) preserves the total energy of the wave packet

$$W = \int_{-\infty}^{+\infty} \sum_{n,m} |u_{n,m}|^2 d\tau = \text{const.} \quad (2)$$

In the case of continuous radiation $\partial_{\tau\tau} u_{nm} = 0$, the conserved quantity is the power

$$\mathcal{P} = \sum_{n,m} |u_{n,m}|^2. \quad (3)$$

To study the peculiarities of the discrete problem qualitatively, we turn to the aberration-free approximation and then compare the results of the approximate analysis with the numerical solution of the system (1). To obtain analytical results, as in [16], we use the approach based on the Lagrangian

$$\mathcal{L} = \sum_{n,m=-\infty}^{+\infty} \frac{i}{2} \left(u_{n,m} \frac{\partial u_{n,m}^*}{\partial z} - c.c. \right) + \left| \frac{\partial u_{nm}}{\partial \tau} \right|^2 - (u_{n+1,m} u_{n,m}^* + u_{n,m+1} u_{n,m}^* + c.c.) - \frac{1}{2} |u_{n,m}|^4. \quad (4)$$

Using the Poisson summation formula

$$\sum \mathcal{F}(n, m, z) = \int \mathcal{F}(x, y, z) \sum e^{2\pi i n x + 2\pi i m y} dx dy, \quad (5)$$

the expression (4) is converted to a form

$$\mathcal{L} = \sum \int \left[\frac{i}{2} \left(u \frac{\partial u^*}{\partial z} - c.c. \right) + \left| \frac{\partial u_{nm}}{\partial \tau} \right|^2 - (u(x+1, y, z) u^*(x, y, z) + u(x, y+1, z) u^*(x, y, z) + c.c.) - \frac{1}{2} |u|^4 \right] e^{i2\pi(nx+my)} dx dy, \quad (6)$$

that allows us to describe the evolution of a discrete system by a function of the continuous argument $u(x, y, z)$. As a result, the problem has been reduced to a ‘‘continuous’’ one, for which analysis is natural to use the aberration-free approximation.

Next, we will study the evolution of axially symmetric Gaussian wave packets

$$u_{n,m} = \frac{\sqrt{W}}{a\sqrt{\tau_0}\sqrt[4]{\pi^3}} \exp \left(-\frac{\tau^2}{2\tau_0^2} - \frac{(x^2 + y^2)}{2a^2} + i\alpha(x^2 + y^2) + i\beta\tau^2 \right). \quad (7)$$

Parameters τ_0 and β characterize the duration and frequency modulation (chirp) of the wave packet. Parameters $a(z)$ and $\alpha(z)$ describe the change of the beam width and the curvature of its phase front during the propagation.

In the considered case of Gaussian field distributions (7), we can integrate in (6) and obtain an expression for the Lagrangian in the form of a functional series. Estimates of the series terms show that it is sufficient to confine oneself to the only one term with $n = m = 0$ to describe the processes with $a \gg 1/\pi$. This condition actually means that the proposed approximation of the discrete field distribution by the continuous function (7) remains valid also for describing the evolution of distributions with a characteristic scale comparable with the lattice size. As a result, we arrive at the following truncated Lagrangian of the system

$$\mathcal{L}_0 = \dot{\alpha} a^2 W + \frac{1}{2} \dot{\beta} \tau_0^2 W + \frac{W}{2\tau_0^2} (1 + 4\beta^2 \tau_0^4) - 4W \exp \left(-\frac{1}{4a^2} - \alpha^2 a^2 \right) - \frac{W^2}{\sigma a^2 \tau_0}, \quad (8)$$

where $\sigma = 4\pi\sqrt{2\pi}$, $\dot{q} \equiv dq/dz$, and q are parameters $\{a, \tau_0, \alpha, \beta\}$. Using the Euler equation

$$\frac{d}{dz} \frac{\partial \mathcal{L}_0}{\partial \dot{q}} - \frac{\partial \mathcal{L}_0}{\partial q} = 0,$$

we obtain

$$\dot{\alpha} = \left(\frac{1}{a^4} - 4\alpha^2 \right) e^{-\frac{1}{4a^2} - \alpha^2 a^2} - \frac{W}{\sigma a^4 \tau_0}, \quad (9a)$$

$$\dot{a} = 4\alpha a e^{-\frac{1}{4a^2} - \alpha^2 a^2}, \quad (9b)$$

$$\dot{\tau}_0 = \frac{4}{\tau_0^3} - \frac{4}{\sigma} \frac{W}{a^2 \tau_0^2}. \quad (9c)$$

The equations (9a), (9c) describe the competition of diffraction (the first terms) and nonlinear refraction (second terms). The nonlinear alteration of the phase front is determined by the same expression as in a continuous medium. The main contribution from the media discreteness is the exponential weakening of the diffraction effects.

Note, equations (9) have a stationary solution with $\alpha = 0$, $\dot{a} = 0$, $\dot{\tau}_0 = 0$ and

$$\mathcal{P} \equiv \frac{W}{\sqrt{2\pi}\tau_0} = 4\pi \exp\left(-\frac{1}{4a_s^2}\right), \quad (10)$$

where a_s is the width of the homogeneous waveguide channel. There are no stationary solutions for $\mathcal{P} > \mathcal{P}_{\text{cr}} = 4\pi$. Exactly this regime of self-action we will consider below. For $\mathcal{P} \leq 4\pi$, the stationary solutions correspond to discrete analogue of Townes mode in continuous media [17]. However, these solutions are unstable according to generalized criteria of Vakhitov-Kolokolov [18], similarly to ones in continuous case.

A. Collapse of 2D wave beams

Let us first consider the stationary wave beam dynamics (i.e. assume $\tau_0 \rightarrow \infty$). In this case, the system of equations (9a), (9b) have the integral

$$\exp\left(-\frac{1}{4a^2} - \alpha^2 a^2\right) + \frac{\mathcal{P}}{16\pi a^2} = \mathcal{C}. \quad (11)$$

In the considered case, \mathcal{C} is a quantity proportional to the Hamiltonian. From the Eq. (11), we can find for the curvature of the phase front

$$\alpha^2 = \frac{1}{a^2} \left[-\ln\left(\mathcal{C} - \frac{\mathcal{P}}{16\pi a^2}\right) - \frac{1}{4a^2} \right]. \quad (12)$$

This expression is meaningful only for wave beams with a size greater than the minimal one

$$a_{\text{min}} = \sqrt{\frac{\mathcal{P}}{16\pi\mathcal{C}}}. \quad (13)$$

In the case of an initial wide collimated wave beam ($a_0 \gg a_{\text{min}}$, $\alpha_0 = 0$), the integration constant is $\mathcal{C} \simeq 1$. It is easy to see that the right-hand side of (12) is positive for the power $\mathcal{P} > 4\pi$. This corresponds to the self-focusing condition in the continuous case.

Excluding α from (9b), we obtain the equation

$$\frac{da}{dz} = \pm 4\left(\mathcal{C} - \frac{\mathcal{P}}{16\pi a^2}\right) \sqrt{-\ln\left(\mathcal{C} - \frac{\mathcal{P}}{16\pi a^2}\right) - \frac{1}{4a^2}}, \quad (14)$$

describing the evolution of the beam width. Its right-hand side contains two cofactors. The spatial dynamics of broad wave beams ($a \gg a_{\text{min}}$) with a power greater than the critical one is determined by the second cofactor. The qualitative difference from a continuous medium arises

with decreasing of beam width and is associated with the role of the first cofactor in Eq. (14). Thus, we can distinguish two evolution stages of wide wave beams ($\mathcal{C} \approx 1$). At the first (while $\mathcal{P} \ll 16\pi a^2$), the radiation self-focusing occurs as in the continuous case. It is described by equation

$$\frac{da}{dz} = -\frac{1}{\sqrt{\pi}a} \sqrt{\mathcal{P} - 4\pi}. \quad (15)$$

Hence, for the self-focusing length, we find

$$L_{\text{sf}} = \frac{a_0^2 \sqrt{\pi}}{2\sqrt{\mathcal{P} - 4\pi}}. \quad (16)$$

During the self-focusing of the beam, the discreteness of the medium begins to count and the system goes into a mode in which the first cofactor in Eq. (14) vanishes.

At this final stage, the evolution of the width is determined by the equation

$$\frac{da}{dz} = -4\left(\mathcal{C} - \frac{\mathcal{P}}{16\pi a^2}\right) \sqrt{-\ln\left(\mathcal{C} - \frac{\mathcal{P}}{16\pi a^2}\right)}. \quad (17)$$

It describes the decrease of the wave beam width as $z \rightarrow \infty$ to the minimum size (13) by the asymptotic law

$$a \approx \sqrt{\frac{\mathcal{P}}{16\pi}} \left[1 + \frac{1}{2} \exp\left(-\frac{256\pi}{\mathcal{P}} z^2\right) \right]. \quad (18)$$

Hence, the characteristic length of a homogeneous waveguide channel formation is much smaller than the self-focusing length (16). The smallness of this length justifies the separation of two stages in the field evolution: self-focusing and formation of a ‘‘homogeneous’’ waveguide structure. It is important to note that the self-channeling mode differs significantly from the continuous one. The phase front of the wave beam in this regime is not flat. From (9a) we see that the wave front curvature increases linearly with respect to z along the propagation path as soon as the width decreases to a minimum size. Thus, this process corresponds more likely to a collapse to the wave beam structure of a finite width.

B. Self-compression of 3D wave packets

Let us now turn to the study of the features of self-compression of laser pulses in a discrete system. In this case it is necessary to analyze the complete, four-dimensional system of equations (9). However, for sufficiently short pulses $\tau_0 \ll a$, we can select a slow motion trajectory in the system (9), which corresponds to a soliton-like field distributions along the longitudinal coordinate. For such distributions, the right-hand side of (9c) is close to zero. This means that the pulse duration changes smoothly during self-focusing of the radiation according to the law

$$\tau_0(z) \approx \frac{\sigma}{W} a^2(z). \quad (19)$$

Excluding τ_0 from (9a), we obtain

$$\dot{\alpha} = \left(\frac{1}{a^4} - 4\alpha^2 \right) e^{-\frac{1}{4a^2} - \alpha^2 a^2} - \frac{W^2}{\sigma^2 a^6}. \quad (20)$$

So, the self-action of soliton-like pulses is described by the equations (9b), (20) having an integral similar to (11)

$$\exp \left(-\frac{1}{4a^2} - \alpha^2 a^2 \right) + \frac{W^2}{2\sigma^2 a^4} = C. \quad (21)$$

As above, the integration constant $C \simeq 1$ for a wide initial collimated wave packet ($a_0 \gg 1$, $\alpha_0 = 0$).

Excluding α from (21) we found the following equation for the wave beam width

$$\frac{da}{dz} = \pm 4 \left(1 - \frac{W^2}{2\sigma^2 a^4} \right) \sqrt{-\ln \left(1 - \frac{W^2}{2\sigma^2 a^4} \right) - \frac{1}{4a^2}}. \quad (22)$$

The situation here is somewhat more complicated than for analogous equation (14) in the two-dimensional case. As above, the evolution of a wide wave packet ($a^2 \gg W/\sigma$) proceeds as in continuous media and is determined by the second cofactor in Eq. (22). However, the critical energy for self-focusing in the three-dimensional case depends on the initial width of the wave beam a_0 :

$$W > W_{\text{cr}} = \sqrt{2}\sigma a_0. \quad (23)$$

If this relation is satisfied then the three-dimensional collapse take place (both the beam width and its duration decreases according to (19)). In the process of self-focusing, the role of the first cofactor in (22), caused by the media discreteness, increases. As a result, the asymptotic law at $z \rightarrow \infty$ is described by equation

$$\frac{da}{dz} = -4 \left(1 - \frac{W^2}{2\sigma^2 a^4} \right) \sqrt{-\ln \left(1 - \frac{W^2}{2\sigma^2 a^4} \right)}.$$

Its solution

$$a = a_c \left[1 + \frac{1}{4} e^{-64z^2/a_c^2} \right], \quad a_c = \sqrt{W/\sigma}. \quad (24)$$

describes the regime of radiation self-focusing up to the characteristic size a_c . In this case, according to (19), an adiabatic decrease in the pulse duration up to the value takes place

$$\tau_c = 1. \quad (25)$$

Thus, the qualitative study shows that the radiation self-focusing is accompanied by a noticeable shortening of the duration of three-dimensional wave packets with a soliton-like distribution along the longitudinal coordinate. At the initial stage, the self-action process develops as in the continuous media and is determined by the same condition (23) [19]. The features of the discrete medium become apparent at the final stage and lead to the finite size of the field localization in the transverse (24) and longitudinal (25) directions. As a result, a localized structure, called *light bullet*, is formed.

III. RESULTS OF NUMERICAL SIMULATION OF WAVE BEAM SELF-FOCUSING

Numerical simulation of the initial equations (1) in media without dispersion shows that the aberration-free approximation quite well describes the features of the discrete problem for a power that is of order of the critical value $\mathcal{P}_{\text{cr}} = 4\pi$. The data presented in figures 1–4 give a complete picture of the evolution of the initially wide (on the lattice scale) Gaussian wave beam (7) with $\alpha_0 = 0$. At a power of \mathcal{P} exceeding the critical self-focusing power \mathcal{P}_{cr} , the radiation is focused and the wave beam is self-channeled near the system axis (see Fig. 1). Data processing shows (see Fig. 4) that the radiation becomes localized in the central fiber for $\mathcal{P} < 10\mathcal{P}_{\text{cr}}$. A further increase of the power of the wave beam is accompanied by an increase of the effective region of self-localization of the field. With increasing radiation power, one can see the development of the filamentation instability and the wave beam splitting (see Fig. 1(c)). In continuous media for a Gaussian field distribution, this process was studied in the papers [20]. It was shown that wave beam splitting develops if the power is an order of magnitude greater than the critical power of self-focusing.

For a discrete system, the necessary conclusions can be drawn from the expression for the growth rate of the Γ filamentation instability of a plane wave with amplitude u_0 . The corresponding Γ dependence on the wave number κ of the perturbation $\propto \exp(i\kappa n)$ has the form [12]

$$\Gamma^2 = 4 \sin^2 \frac{\kappa}{2} \left(2u_0^2 - 4 \sin^2 \frac{\kappa}{2} \right). \quad (26)$$

It follows that the instability growth rate for $u_0^2 > 2$ is maximal at the transverse scale of the field perturbation equal to the lattice period

$$L_{\perp} \equiv \pi/\kappa = 1 \quad \text{for} \quad u_0 > \sqrt{2}. \quad (27)$$

The numerical simulation demonstrates splitting of self-channeled radiation with the fields amplitudes $u_0 \gg \sqrt{2}$. Thus, the development of filamentation instability in a discrete problem leads, at a nonlinear stage, to the wave beam splitting into a set of wave structures localized in separate optical fibers. The corresponding soliton-type distributions were investigated in the papers [21, 22].

The fields in each fiber will have their own nonlinear frequency shift $\delta\omega \simeq |u_{n,m}|^2$, according to (1). The interaction between the light guides will be exponentially weak if the phase difference $L_d(\delta\omega - \delta\omega') \simeq L_d|u||L_{\perp}\nabla u| \approx L_d|u|^2$ for the characteristic “diffraction” length of one lattice cell $L_d \simeq 1/2$ is much larger π . At a nonlinear stage, this limits the growth of the field amplitude by the magnitude of the order of $\max|u| \gtrsim \sqrt{2\pi}$, which is confirmed by the results of numerical simulation (Fig. 2). Moreover, the same process will weaken the spreading of the wave field during long-term evolution (Fig. 2(c)-(d)). Along with the filamentation in the central part, the focusing continues at the periphery of

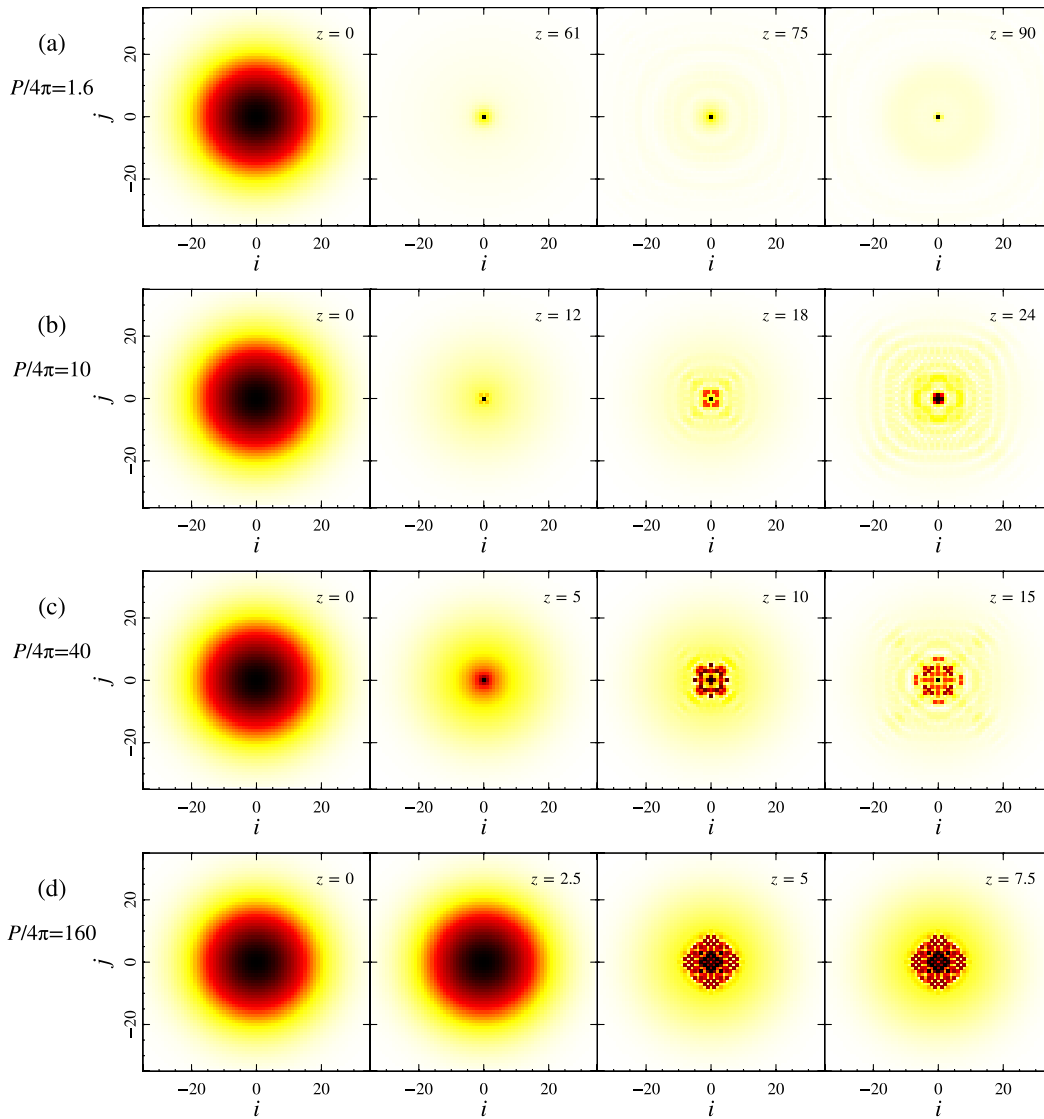


Figure 1. (Color online) Evolution of the amplitude distribution of a wave beam during its self-focusing in a discrete medium.

the wave beam. This is responsible for some growth of the region occupied by the intense field $a_{1/2}$ immediately after the collapse point.

Finally, the presence of instability only in a localized region leads to the appearance of a complex, stochastic field dynamics for powers significantly exceeding the critical one. Both the modification of the stratified structure as the wave field propagates, and the presence of strongly localized maximum at $\delta z = 0$ (Fig. 3(a)) in the autocorrelation function testify to this. Autocorrelation functions are defined as follows: $K_{ij}(\delta z) = \int (u_{ij}(z)u_{ij}^*(z + \delta z) + c.c.) dz$ and $K_{\perp}(\delta i, \delta j) = \sum (u_{ij}u_{i+\delta i, j+\delta j}^* + c.c.)$ for evolutionary and transverse coordinates correspondingly. The number of inhomogeneities can be estimated as follows. Numerical simulation of the excitation of an individual light-guide shows that for an initial value of the field in an isolated light-guide larger than 6, the nonlinear

contribution to the field evolution becomes stronger than the tunneling of the wave field into neighboring fibers and self-channeling of the radiation in it takes place. Thus, for the radiation parameters in Fig. 1(c), one should expect the excitation of about 20 inhomogeneities, which corresponds to the data of numerical simulation. Moreover, such inhomogeneities are incoherent, since their spatial autocorrelation function is strongly localized near the zero (Fig. 3(b,c)).

Another noticeable difference between the discrete problem and the continuous one is associated with the diffusion of the wave field into the peripheral region during the radiation self-focusing. In the one-dimensional case, this effect is described in [16]. Its magnitude in the two-dimensional problem under consideration can be judged from Fig. 2, which shows the change in power in the central part of the wave beam (at 1/2 level) along

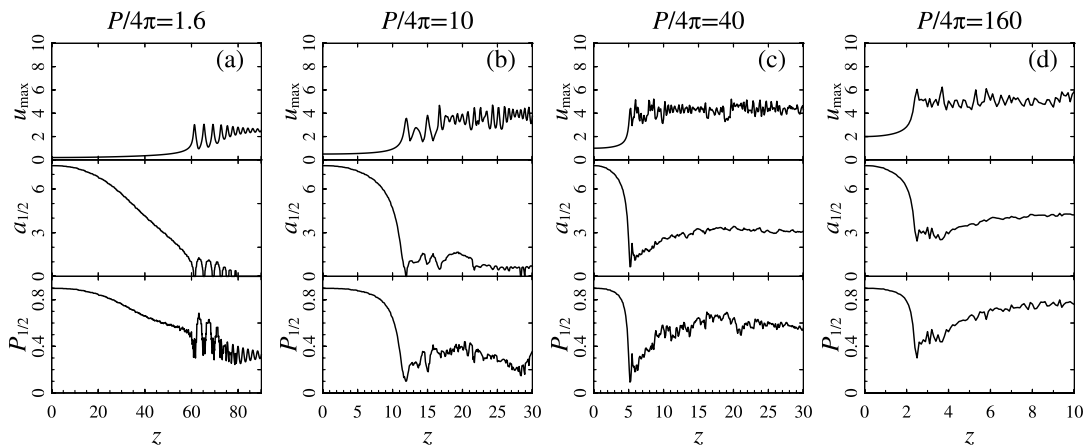


Figure 2. The maximum amplitude u_{\max} , the width $a_{1/2}$ and the power fraction $P_{1/2}$ in fibers with a high intensity depending on the evolution variable z for different initial power \mathcal{P} . The limitation of the maximum amplitude, associated with the development of the filamentation instability, is seen.

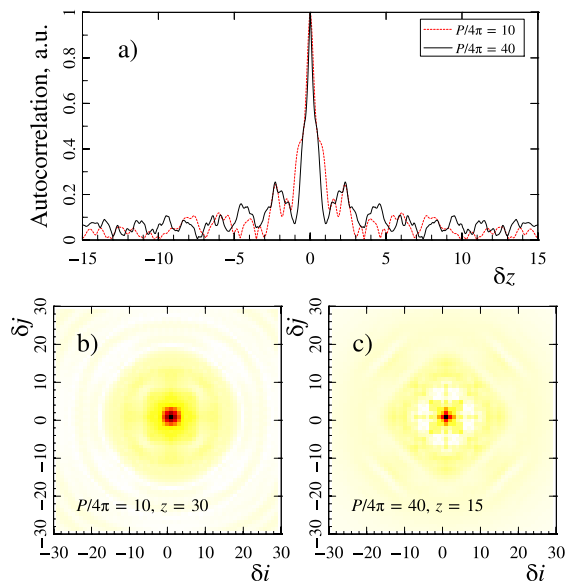


Figure 3. (Color online) Autocorrelation function for the wave field envelope along evolutionary coordinate in the central fiber (a) and along transverse coordinates (b, c) for different power values.

the propagation path. In self-trapping mode, about half of the initial power is captured (see figure 2). Note, the captured power remains greater than the critical power of self-channeling even in the worst case (see Fig. 2(a)).

At a power exceeding \mathcal{P}_{cr} by an order of magnitude, a typical aureole appears (see Fig. 1). This region has a characteristic size comparable to the width of the original wave beam. The peripheral part of the wave field weakens somewhat on the propagation path as it moves away from the focal region. As a result, as seen in Fig. 2(c), there is an increase of both the power fraction in the axial part and the characteristic size of the intense field region with

increasing wave beam power. Simultaneously a certain increase of the field amplitude on the axis of the system (see Fig. 4), a widening of the field localization region and a shortening in the self-focusing length take place in agreement with the aberration-free approximation (15).

IV. LIGHT BULLETS FORMATION

The collapse of three-dimensional wave packets, even within the framework of continuous NSE, belongs to the number of insufficiently investigated processes [23], especially in the case of wave packets, which are oblate in longitudinal direction [19]. The specificity of the problem we are considering is that, the media discreteness begins to affect as the wave field becomes self-focusing, and it becomes possible to capture radiation into the self-channeling regime (see section II B).

Numerical simulation of the evolution of wave packets with initial Gaussian form shows that the process of radiation self-focusing and pulse self-compression develops in accordance with the aberration-free approximation. The decrease in pulse duration in the process of self-focusing (Fig. 5) occurs according to the law (19). So, we can obtain from (22) the following estimate for the self-focusing length

$$L_f = \frac{a_0^3 2\pi^{3/4}}{3W}. \quad (28)$$

It is clear from figures 6 and 7 that the light bullet is formed at this length and then the radiation propagates in the self-channeling mode.

A strong increase of the field in the near-axis region creates conditions for the development of a modulation instability. The situation here is the same as in the radiation propagation in a single fiber. One can see on figure 6 the splitting of the wave packet into a set of soliton-type

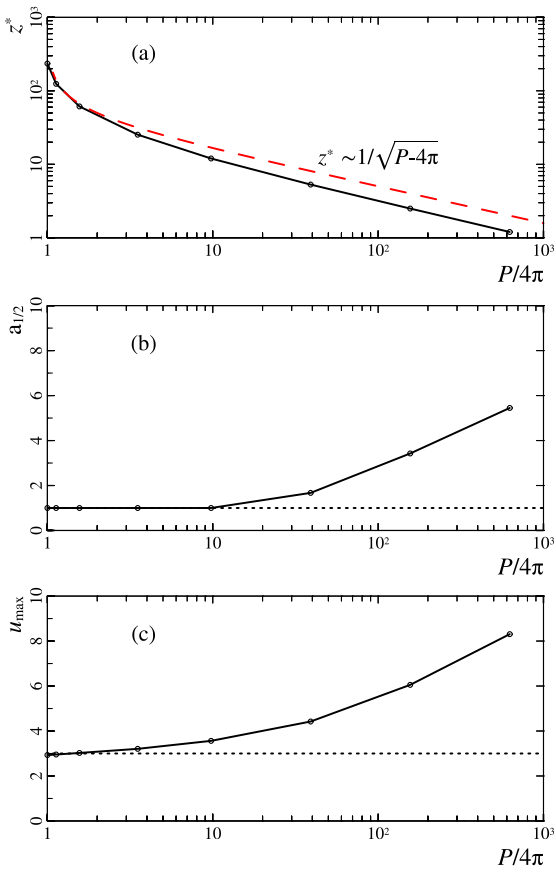


Figure 4. **(a)** Dependence of the length of self-focusing on wave beam power. The dashed curve corresponds to the analytical expression (16), a solid one is the result of numerical simulation. Figures **(b,c)** show the dependence of the effective localization region $a_{1/2}$ and the maximum value of the field amplitude u_{\max} on the power \mathcal{P} . The dotted lines represent: the minimum lattice period **(b)** and the amplitude threshold at which the applicability of the aberration-free approximation **(c)** is violated.

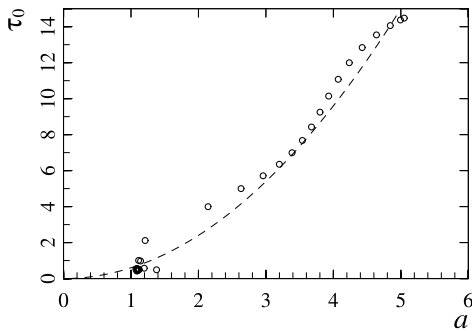


Figure 5. Dependence of the wave packet duration τ_0 on its width a during self-focusing process. The dashed curve is described by the formula (19) for $W = 315$. A curve consisting of hollow circles is determined on the basis of numerical simulation data of the original equation (1). Initial wave packet form is $u_{n,m} = 0.4e^{-(n-25)^2 + (m-25)^2/50 - \tau^2/400}$.

structures self-channeled in the central waveguide and the formation of three light bullets. The development of modulation instability naturally limits the propagation of fields, with an amplitude greater than the critical one, in fiber systems. As above (section III), the wave field is ejected into the peripheral region in while passing from radiation self-focusing to self-channeling. It can be seen from figure 7 that it is about half the total energy. The behavior of the characteristic parameters of the spatial part of the field (see Fig. 7) gives a picture that is similar in many aspects to one of wave beam self-focusing (Fig. 2). As for the duration of the wave packet, we see in figure 7 a monotonic decrease of this parameter for self-focusing according to the law (19) (see also Fig. 5).

However, as the radiation is self-focused to a size of the order of the lattice period, a violation of the (19) law and the development of the modulation instability occur because of the appearance of aberrations in the wave packet due to the media discreteness. Numerical simulation of self-action shows that it is not possible to suppress the effects of modulation instability under conditions of enhanced filamentation with increasing energy in the pulse for the case of wave packets with initially Gaussian shape. Forming a set of light bullets in longitudinal direction is not a very good scenario. The task of summation the sequence of laser pulses at the output from a nonlinear medium for the purpose of further use is a complicated problem. It is a different matter in the case of the predominant development of transverse filamentation and the subsequent formation of light bullets flying parallel to each other. Such an opportunity can, for example, be realized with axicon focusing in a system of coupled light guides [24]. This is due to the fact that in the Bessel wave beams the inhomogeneities of the transverse structure are much more pronounced than in the Gaussian ones.

Let us consider the possibility of the predominant development of the transverse filamentation of the wave field ahead of the longitudinal modulation in the problem of the plane wave instability. The generalization of the instability growth rate (26) to the case allowing for the additional weak longitudinal modulation with the scale $2\pi/\Omega$ leads to the following expression

$$\Gamma^2 = \left(\Omega^2 + 4 \sin^2 \frac{\kappa}{2} \right) \left(2u_0^2 - \Omega^2 - 4 \sin^2 \frac{\kappa}{2} \right). \quad (29)$$

Hence, discrete symmetry with respect to longitudinal and transverse perturbations is violated unlike a continuous medium. The characteristic scales of the perturbations $2\pi/\Omega_0$, $2\pi/\kappa_0$ for which the instability growth rate (29) is maximal are determined from the following relations

$$\sin \frac{\kappa_0}{2} \cos \frac{\kappa_0}{2} \left(u_0^2 - \Omega_0^2 - 4 \sin^2 \frac{\kappa_0}{2} \right) = 0 \quad (30a)$$

$$\Omega_0^2 + 4 \sin^2 \frac{\kappa_0}{2} = u_0^2. \quad (30b)$$

As in the section III, it is natural to assume that the spatial inhomogeneity of the medium defines the charac-

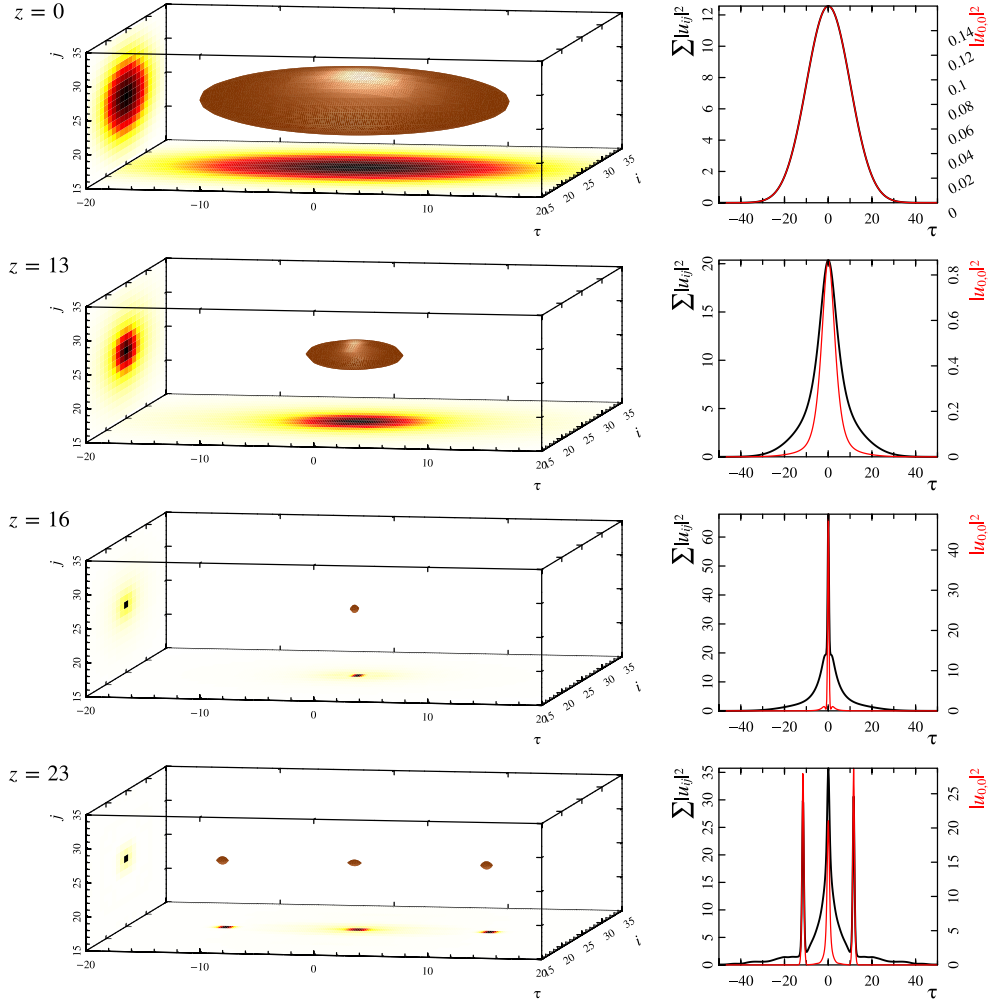


Figure 6. (Color online) The left column shows the amplitude distributions of wave packet with energy exceeding the critical one at different values of z . The right column shows the corresponding time structures of the wave packet: integral one (black) and one in the region of the maximum field (red).

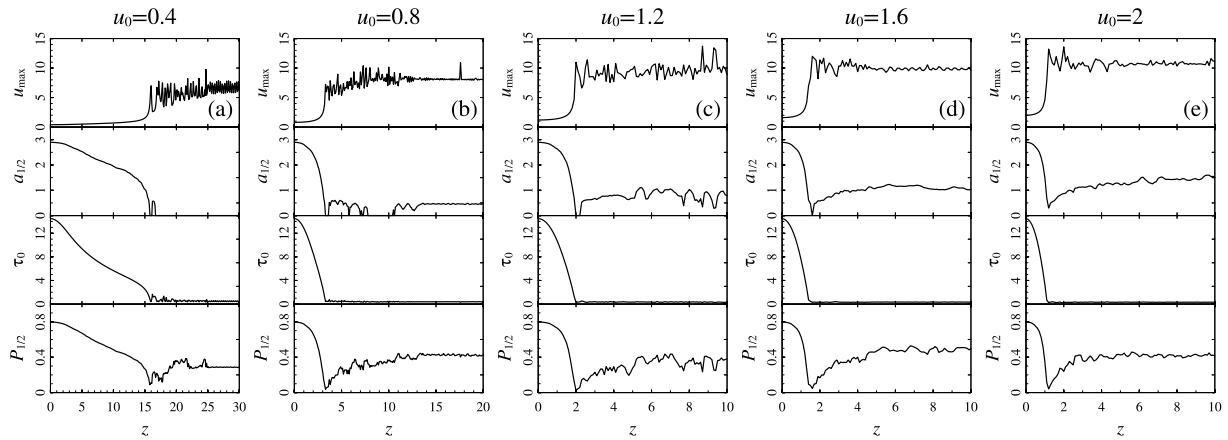


Figure 7. The maximum amplitude u_{\max} , the width $a_{1/2}$, pike duration and the power fraction $P_{1/2}$ in fibers with a high intensity depending on the evolution variable z for different initial field amplitude u_0 . It is seen that limitation of the maximum amplitude, associated with the development of the modulation instability. In addition, one can see the lack of focusing in single channel at the amplitude of $u_0 = 0.8$ and higher.

teristic spatial scale of the perturbations $\cos(\kappa_0/2) = 0$ (see Eq. (27)). In this case, we find for the longitudinal wave number from (30b)

$$\Omega_0^2 = u_0^2 - 4. \quad (31)$$

So, the development of the modulation instability is stabilized for fields $u_0 < 2$ and the transverse filamentation becomes dominant, which develops as in the section III. The upper field limit ($u_0 < 2$) is violated during the self-focusing and subsequent self-channeling of Gaussian wave beams (see Fig. 7). We suggest to use hollow wave packets for avoiding excitation at transportation of high total power.

The results of numerical simulation of wave packets of the form

$$u_{n,m} = u_0 e^{-\left(\sqrt{(n-25)^2 + (m-25)^2} - r_0\right)^2 / 50 - \tau^2 / 400} \quad (32)$$

are shown in the figures 8 and 9. It is seen from Fig. 9, that the self-focusing mode depends on the field amplitude. Thus, an increase of the field amplitude from $u_0 = 0.4$ to $u_0 = 0.8$ at $r_0 = 5$ leads to a change in the structure of the focal region. At $u_0 = 0.4$, the radiation self-focusing takes place on the axis of the system as in continuous case. The hollow structure of the wave packet is preserved if the field amplitude is doubled. In this case, the self-focusing of the radiation is accompanied by an increase of the field on the ring, somewhat less than the initial radius (see Fig. 9), which weakens the maximum attainable value of the field amplitude. In the process of forming of an annular beam with a characteristic thickness close to the lattice period, the laser pulse is shortened, and the field filamentation occurs only along the angular variable. The corresponding field evolution is shown in Fig. 8. One can see the formation of light bullets located on the ring and flying parallel to the axis of the system. The fifth part of the original energy is involved in this process.

As such stratified structure propagates, the pulse duration decreases. The analysis of numerical simulation results show that these wave structures have equal phases only in certain groups of optical fibers located on the ring. This is due to the symmetry of the square structure of considered array of fibers. Figure 10(a) schematically shows three groups of light-guides (black solid circles, squares and rhombus) in which the wave structures are mutually in-phase. It should be noted that the fraction of energy contained in the group of optical fibers marked by black circles is noticeably larger than in the other groups. Figure 10(b) shows the time distributions of the laser pulses for three different cases. The blue dash line shows the wave packet profile, which is result of the summation $\sum |u_{ij}|^2$ of the intensities over all light guides. Solid black curve shows the time profile of coherent field from the group of light-guides, marked by black circles (see Fig. 10(a)). It is important to note, that the amplitude of the output signal does not depend on the interaction length after the formation of light bullets. Unfortunately, the wave field frequencies in different

groups of light-guides are slightly different. This results in variation of the coherently summed amplitude of wave fields on the ring in dependence on the interaction length. The shaded area in Fig. 10(b) shows the scatter of these profiles. It can be seen that the intensity of the coherent output signal in this case depends on the length of the light-guides. However, even in the worst case, the intensity of the coherent radiation is higher than the total ‘‘incoherent’’ intensity from all the light guides.

Thus, it is possible to gather the field with from the group of light-guides, marked by black circles, using linear elements (for example, a lens) at the output of the system. This forms laser pulse which are much shorter and intense, than the original one. As it follows from Fig. 8 and 10(b), the laser pulse duration decrease by a factor of 15 during considered self-action process. Its intensity increase more than 500 times. At this, the summed output pulse contains more than 25% of the energy of the initial pulse.

V. CONCLUSION

The study of self-action of wave packets propagating along a two-dimensional system of coupled light-guides shows that the media discreteness leads to new features in the evolution of the system. To construct a qualitative picture, we developed an aberration-free approximation within the framework of the variational approach. Due to its use, we classified the self-action regimes, determined the characteristic parameters, and described the transition of self-focusing of wide wave beams to the self-channeling mode in the central fiber. This process reflects the peculiarities of a discrete medium and does not depend on the dimension of the problem.

A more detailed study of the wave field collapse and its subsequent self-channeling in the near-axis region was carried out on the basis of numerical simulation of a discrete NSE. The analysis of the self-focusing of wide axially symmetric wave beams has shown that the aberration-free self-action regime takes place in a limited range of powers exceeding the critical one for self-focusing. The process of beam collapse is accompanied by the emission of a wave field from the near-axis region. Losses are up to half of the original power under conditions of a small excess over the threshold value. At powers exceeding the critical power of self-focusing by a factor of ten, the development of filamentation instability becomes a noticeable process. Unlike a continuous medium, instability develops in a nonlinear focal region, where the field intensity increases strongly. The characteristic scale of the instability is equal to the lattice period of discrete medium and doesn't depend on the field amplitude for amplitudes above the threshold (27). As a result, the further propagation of radiation occurs through a set of fibers in the self-trapping mode.

The analysis of transition of laser pulse self-compression to its self-channeling shows the possibil-

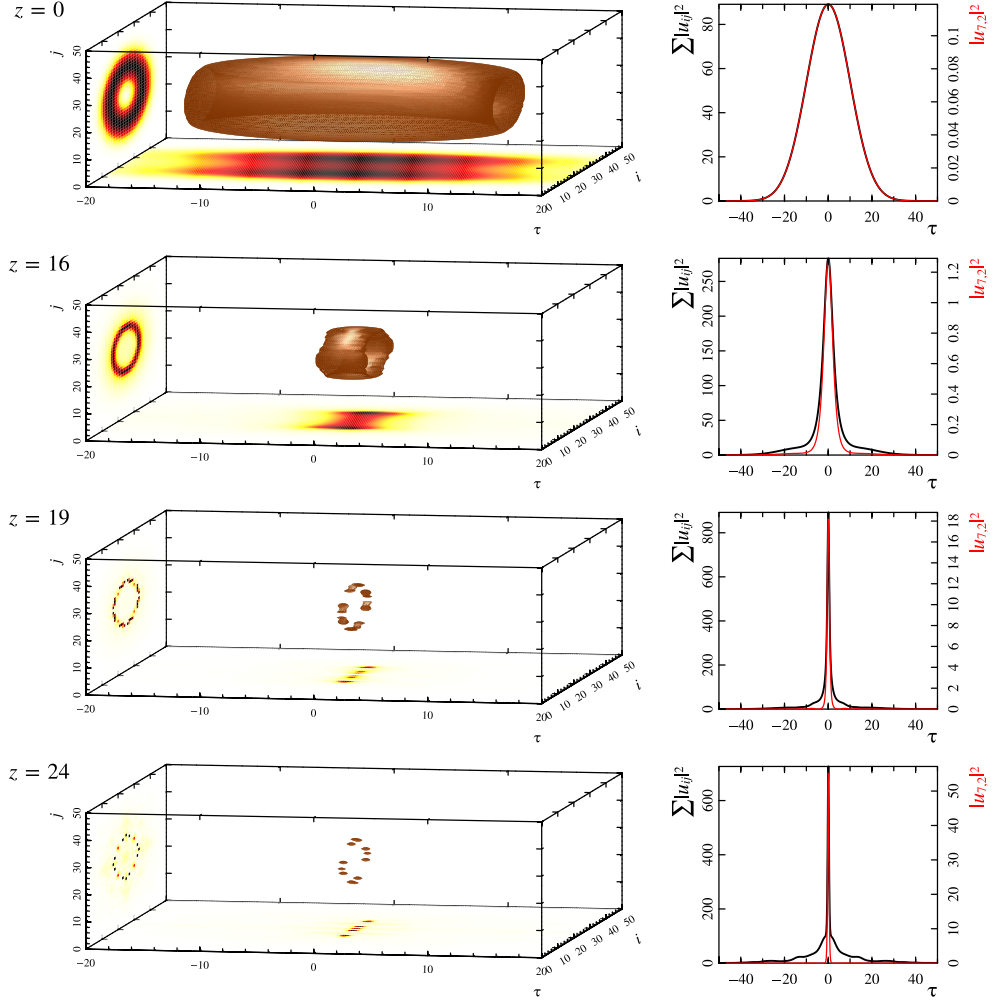


Figure 8. (Color online) The left column shows the amplitude distributions of hollow wave packet at different values of z . The right column shows the corresponding time structures of the wave packet: integral one (black) and one in the region of the maximum field (red).

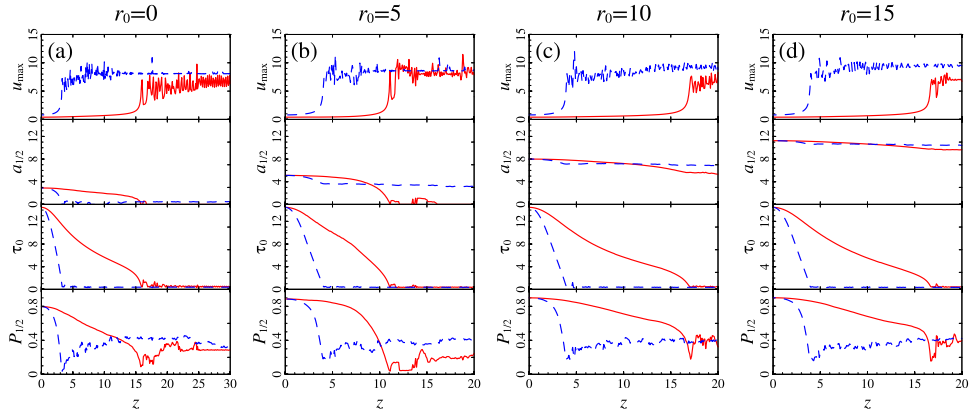


Figure 9. (Color online) Dependences of the maximum amplitude u_{\max} , the width $a_{1/2}$, pike duration and the power fraction $P_{1/2}$ in fibers with a high intensity depending on the evolution variable z for different initial ring radius r_0 with field amplitude $u_0 = 0.4$ (solid) and $u_0 = 0.8$ (dash). There is no collapse of the wave packet to the center fiber both for large initial amplitudes (b) and for a large radius of the ring (c,d).

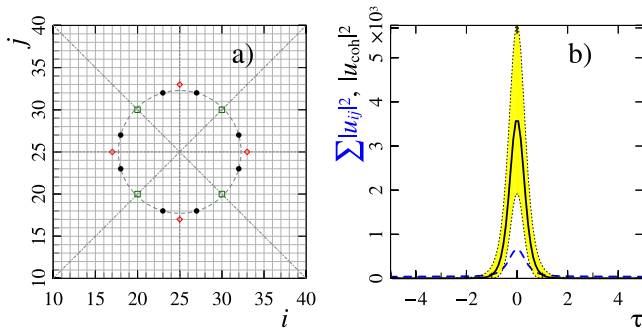


Figure 10. (Color online) Coherent groups of light-guides (a) and result of coherent summation (b) of wave field over most intensive light-guides (black solid circles in (a)) for parameter of Fig. 8. The dash line in figure (b) is result of incoherent summation of wave intensity over the whole region. The shaded area shows the change in the coherent intensity depending on the interaction length.

ity of a noticeable decrease in the duration of a three-dimensional wave packet. However, as the self-focusing and localization of the radiation in the central light-guide increase, the field amplitude increases so much that the non-aberration approximation becomes inapplicable due

to the development of the modulation instability. As a result, the self-channeled compressed wave field splits, as in the one-dimensional continuous case, into a set of solitons. Thus, the self-action of pulsed radiation in a discrete medium with an anomalous dispersion of the group velocity leads to the formation of light bullets flying one-by-one along the system axis.

For practical use, the mode of forming of light bullets that fly parallel to each other is more convenient. Such situation can be realized under conditions when the filamentation instability develops faster than the modulation one. Hollow wave structures are suitable here. Self-focusing of such field distributions leads to a spatial localization of the wave packet near the ring. Numerical simulation shows that as a result of the development of filamentation instability along the angular variable, a set of light bullets is formed in the optical fibers located parallel to the axis of the system. In the process of self-action, the duration of the initial pulse also decreases. More importantly, solitons in individual fibers are coherent. Using linear elements (for example, a lens), the fields at the output of the system can be summed and form much shorter, than the original, intense laser pulse.

This work was supported by the Russian Science Foundation (Project No. 16-12-10472).

-
- [1] Yu. S. Kivshar and G. P. Agrawal, *Optical Solitons: From Fibers to Photonic Crystals* (Academic, San Diego, CA, 2003; Fizmatgiz, Moscow, 2005).
- [2] *Nonlinearities in Periodic Structures and Metamaterials*. Editors: Cornelia Denz, Sergej Flach, Yuri Kivshar. Springer, 2010. ISBN 978-3-642-02066-7.
- [3] A.K.Sarychev, V.M.Shalaev, *Electrodynamics of Metamaterials*, World Scientific Publishing, Singapore (2007).
- [4] Truong X. Tran, Dung C. Duong, and Fabio Biancalana, *Phys. Rev. A* **89**, 013826 (2014).
- [5] A. B. Aceves, G. G. Luther, C. De Angelis, A. M. Rubenchik, and S. K. Turitsyn, *Phys. Rev. Lett.* **75**, 73 (1995).
- [6] A.M. Rubenchik, I.S. Chekhovskoy, M.P. Fedoruk et al., *Optics Letters*, **40**, 721 (2015).
- [7] Boris A. Malomed, *Soliton management in periodic systems*, Springer (2006).
- [8] S. Minardi, F. Eilenberger, Y. V. Kartashov, A. Szameit, U. Röpke, J. Kobelke, K. Schuster, H. Bartelt, S. Nolte, L. Torner, F. Lederer, A. Tünnermann, and T. Pertsch, *Phys. Rev. Lett.* **105**, 263901 (2010).
- [9] Truong X. Tran, Dung C. Duong, and Fabio Biancalana, *Phys. Rev. A*, **90**, 023857 (2014).
- [10] G. Mourou, T. Tajima, M. N. Quinbn, B. Brocklesby, J. Limpert. *Nuclear Instruments and Methods in Physics Research A*, **740**, 17 (2014); G. Mourou, B. Brocklesby, T. Tajima, J. Limpert. *Nature Photonics* **7**, 258 (2013).
- [11] F. Lederer, G. I. Stegeman, D. N. Christodoulides, G. Assanto, Moti Segev, Yaron Silberberg, *Phys. Reports* **463**, 1 (2008).
- [12] O. M. Braun and Yu. S. Kivshar, *The Frenkel-Kontorova Model: Concepts, Methods, and Applications* (Springer, Berlin, 2004; Fizmatlit, Moscow, 2008).
- [13] A. Scott, *Nonlinear Science: Emergence and Dynamics of Coherent Structures* (Oxford Univ. Press, Oxford, 2003; Fizmatlit, Moscow, 2007).
- [14] P. G. Kevrekidis, *The Discrete Nonlinear Schrödinger Equation: Mathematical Analysis, Numerical Computations and Physical Perspectives* (Springer, Berlin, 2009).
- [15] A. Trombettoni and A. Smerzi, *Phys. Rev. Lett.* **86**, 2353 (2001).
- [16] A. A. Balakin, A. G. Litvak, V. A. Mironov, and S. A. Skobelev, *Phys. Rev. A* **94**, 063806 (2016).
- [17] R.Y. Chiao, E. Garmire, C.H. Townes, *PRL* **13**, 469 (1964).
- [18] E.W. Laedke, K.H. Spatschek, V.K. Mezentsev, S.L. Musher, I.V. Ryshenkova, S.K. Turitsyn, *JETP Lett.* **62**, 677 (1995).
- [19] A.A. Balakin, A.V. Kim, A.G. Litvak, V.A. Mironov, S.A. Skobelev, *Phys. Rev. A* **94**, 043812 (2016).
- [20] G. Fibich, B. Ilan, *Physica D* **157**, 112 (2001).
- [21] V.K. Mezentsev, S.L. Musher, I.V. Ryzhenkova, S.K. Turitsyn, *JETP Lett.*, **60**, 829 (1994).
- [22] N. K. Efremidis, D. N. Christodoulides, and Kyriakos Hizanidis, *Phys. Rev. A* **76**, 043839 (2007).
- [23] *Self-focusing: Past and Present*, R.W. Boyd, S.G. Lukishova, Y.R. Shen (Eds.), *Topics in Applied Physics* **114**, (Springer, New York, 2009).
- [24] A.A. Balakin, V.A. Mironov, S.A. Skobelev, *JETP* **124**, 49 (2017).